Adaptive Adjustment of a Precision Truss Structure: Experimental Validation

M. Salama, J. Umland, R. Bruno, J. Garba
Jet Propulsion Laboratory
California Institute of Technology
Pasadena, California 91109

Abstract

Previous analytical studies have shown the feasibility of using a limited number of active members to adaptively alter the structural shape or behavior to other desired states. As a demonstration of this concept, this paper describes the results of a sequence of validation tests, their correlation with the analytical results, and the problems encountered. An existing full scale, space erectable, high precision truss structure was used.

For the most part, the results showed good agreement with the analysis. However, micron level nonlinearities in the structural behavior were discovered. The significance of the presence of these nonlinearities in precision structures and their impact on the basic premise of adaptivity are discussed.

1. Introduction

Adaptive structure concepts offer unique design alternatives to the designers of proposed filled aperture space based astronomy missions, such as the Sub millimeter Intermediate Mission (SMIM), and the Large Deployable Reflector (LDR). These missions are intended to observe the infrared and sub millimeter wavelengths. They employ a large segmented filled aperture reflector supported by a truss structure. A requirement of a diffraction limited telescope is that the telescope wavefront error be on the order of $\lambda/10$, where λ represents the minimum wavelength of interest. The corresponding reflective surface error requirement is then determined to be half the wavefront error,i.e. $\lambda/20$. Typically, ninety percent of the surface error budget is allocated to the primary reflector. Thus the primary reflector's surface accuracy must be less than 1/20 to 1/25 of the shortest wavelength of interest. Therefore, for missions such as SMIM and LDR, where the wavelengths of interest fall in the 100 - 1000 micron range, the primary reflector's surface accuracy requirement is on the order of a few microns.

A segmented reflector's surface accuracy is to a large extent determined by the dimensional accuracy of the structure supporting it. This is because the reflector panels, which are made to within 'one' micron rms of their correct figure, are positioned above the support structure by a panel actuation mechanism. Therefore, the minimum achievable reflector surface figure error is potentially limited by the range of motion of the panel actuators coupled with the accuracy of the reflector support structure. The advantage of an adaptive structure approach in this context is that, by strategically placing actuators in the support structure, the shape of the support structure can be adjusted to minimize errors produced by finite fabrication precision and/or thermal deformations. Another advantage is that the same actuators may be used to prestress the joints of the support structure in order to remove nonlinearities that may exist due to small free play in the joints.

The shape control of truss structures has been studied by several investigators. For example, in Ref. [1], optimization of the support truss was formulated so as to minimize the required effort to correct the shape, while improving the performance of the antenna. Minimization of the effort required for shape correction was implemented in the form of minimizing the maximum actuator input. This had the effect of equalizing the corrective force among all actuators. And rather than considering the optimal actuator placement as part of the formulation, Ref. [1] used many fixed actuators. An approach for the optimal actuator placement was considered in [2], by first converting a discrete truss structure model into a continuum model, for which the optimum placement is sought. The idea of using an equivalent continuum model is beneficial in that the computational costs of optimization are reduced in comparison to discrete programming methods. However, applicability of the results from the continuum model to the discrete structure is not straight forward.

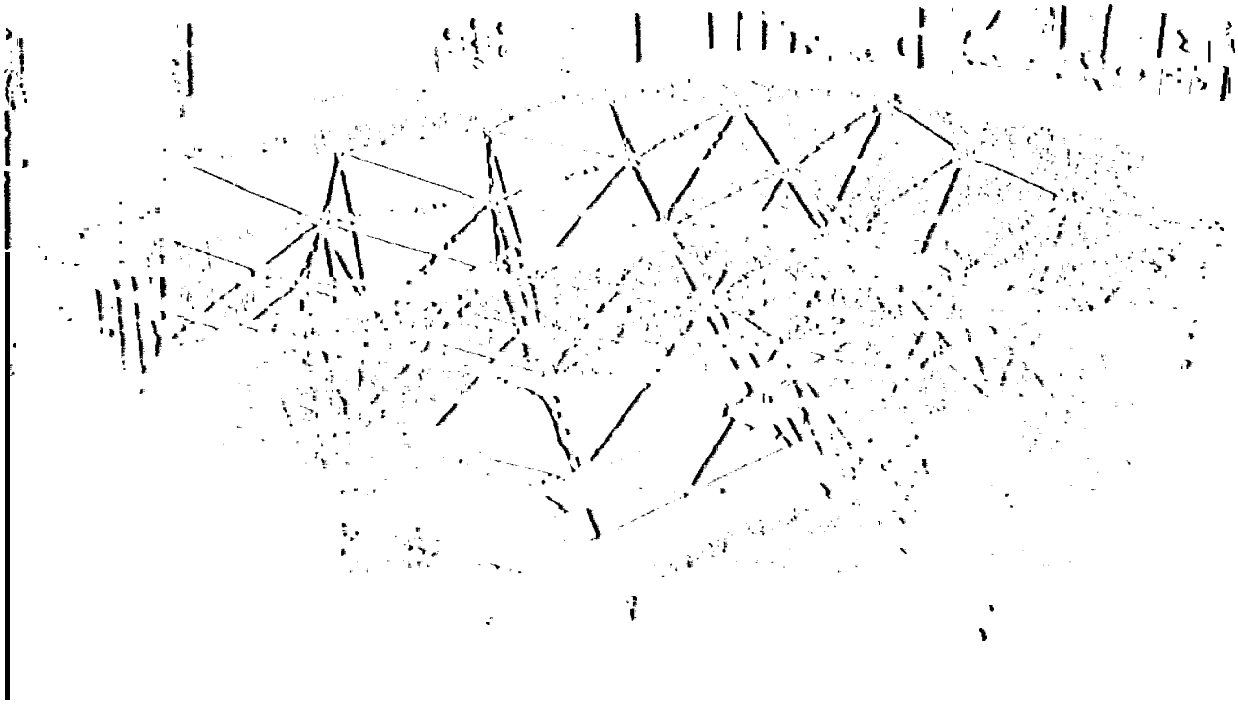

igure 1 recision truss estbed

As an alternative to rigorous discrete optimization methods, heuristic techniques have been suggested and successfully used for the optimal placement problem [3,4,5] - without incurring high computational costs. Specifically, Ref. [5] has employed the simulated annealing technique to minimize shape distortions as well as the effect of nonlinear joint behavior, while using a limited number of actuators. Prestressing or preloading the truss structure or its joints was also studied [6] with the objective of removing any joint nonlinearities. All of these analytical results confirmed the feasibility of using active members to adaptively alter the shape of the structure and/or it's behavior to other states.

Experimental shape control has concentrated mostly on the field of adaptive optics, where the figure of flexible mirrors was controlled by a discrete number of actuators. For example, limited testing was performed [7] to verify the ability of piezoelectric actuators to create a predetermined deformed shape of a composite panel. Also, nine precision force actuators were used [8] to adjust the figure of a 62 cm diameter thin spherical mirror.

Using a space - erectable truss structure, Fig. (1), the objective of his paper is to verify the analytical predictions of Ref. [5] with regard to the ability of a limited number of actuators to correct structural shape aberrations. The structure is a four-meter diameter, doubly curved tetrahedral erectable truss, which has been the subject of considerable previous development and testing.

In the sections that follow, the analysis procedure will be first summarized along with the analytical results which the tests will aim to verify. We will then describe the testbed structure, its active components, instrumentation, and data acquisition system used. Detailed discussion of the test sequence, results, their comparison with the analytical predictions, and the major lessons learned will conclude the paper.

II. Analysis

For the precision structure in Fig. (1), static distortion of the shape can result from: (1) thermal changes and/or gradients due to exposure to sun and shade, (2) the absence of gravity when the structure has been constructed, tested, and analyzed on-ground, and (3) the finite manufacturing tolerances employed. But aside from the source of aberrations, the aim here is to establish the degree to which a limited number of strategically located actuators can realign the

structural shape to a desired configuration.

Shape correction for statically indeterminate truss structures was examined in [5], assuming linear as well as nonlinear joint behavior. In both cases, the objective of the analysis was to find the best locations and gains for a given number of actuators so that a prescribed distortion can be corrected. The actuator gain is defined here as the amount of travel or displacement in an extensible axial member, i.e. an active member. To generate a realistic distorted shape of the structure in Fig. (1), a finite element analysis was first performed to calculate the deformations at all degrees-of-freedom (d.o.f.) of the truss due to a representative 5° K/m thermal gradient inplane in the Y-direction. Subsequent analyses then addressed the problem of the number of actuators, their optimal locations, and gains required to minimize this initial distortion in the Z-direction at the top nodes (or control degrees-of-freedom) of the truss. This is equivalent to athermalizing the structure. But, rather than requiring the actuators to restore the distorted structure to its original shape, we may view the given distortion as the deformation pattern which we desire the actuators to generate.

Detailed description of the analysis can be found in [5], and is therefore given here in brief form for completeness. Let u^* = the vector of desired deformations at a specified set of n_c control points (i.e. control d.o.f.), and u = the vector of deformations induced at the same control d.o.f. by n_ε active members which have been arbitrarily placed and their gains arbitrarily set to Λ_o. For any such a set of actuators, we adopt the rms error functions, ε, as a measure of the actuators ability to achieve the desired shape corrections:

$$\varepsilon = \left[(u^* - u)^T (u^* - u) \right]^{1/2} \qquad (1)$$

Then the optimal actuator locations and gains are those that minimize ε with respect to all possible locations and gains.

In a linear structure, the nodal deformations u at n_c d.o.f. are related to the gains Λ_o by:

$$u = S\Lambda_o \qquad (2)$$

$$S = B_c K_G^{-1} \beta^T K B_\varepsilon \qquad (3)$$

Generally the matrix S is rectangular $n_c \times n_\varepsilon$. If n is the total number of d.o.f., and m is the total number of members in the truss, the remaining matrices in Eq. (3) have the meanings: B_c is $n_c \times n$ matrix of zeros and ones which selects the rows associated with the control d.o.f. in question, B_ε is $n \times n_\varepsilon$ matrix of zeros and ones which selects the columns associated with the actuator locations, K is a diagonal stiffness matrix containing the elemental stiffness EA/L, β is a geometric matrix that relates all the nodal d.o.f. to the length changes in all members of the truss, and $K_G = \beta^T K \beta$ is the system global stiffness. The inverse form of Eq. (2) may be expressed by:

$$\Lambda_o = (S^T S)^{-1} S^T u \qquad (4)$$

Minimization of Eq. (1) with respect to all possible locations and gains, may be performed iteratively within the framework of the simulated annealing algorithm. During a typical simulated annealing iteration i, a new set of locations L_i for the n_ε actuators is generated and the following steps are performed:

a. For the current locations, calculate S_i from (3).

b. Assuming $u_i = u_i^*$, compute approximate set of gains Λ_{oi} from the inverse relationship in (4).

c. From the forward solution in (2), use the results of (a) and (b) to find u_i.

d. Evaluate ε_i from (1).

e. Depending on the relative magnitude of ε_i and ε_{i-1}, and other parameters in the annealing algorithm, the locations L_i may be either accepted or rejected.

f. Stop if minimization of ε has converged, or generate a new L_{i+1} set of locations and go to (a).

The analysis procedure described above was applied [5] to the truss structure of Fig. (1). Some of the main results are summarized in Fig. (2), which shows the rms error correction, ε, that can be achieved using various number of optimally placed actuators. The magnitude of the initial rms error is that shown when $n_\varepsilon = 0$, i.e. no actuators used. Two important observations can be made in connection with Fig. (2):

i. For a statically indeterminate structure with n deformable d.o.f. and m members - where n<m - one needs at least n actuators to exactly produce any desired shape at all n d.o.f. Locations of the n actuators must, however, be optimally selected from among all possible m member locations. Fewer d.o.f. in the desired set allow one to use fewer number of actuators.

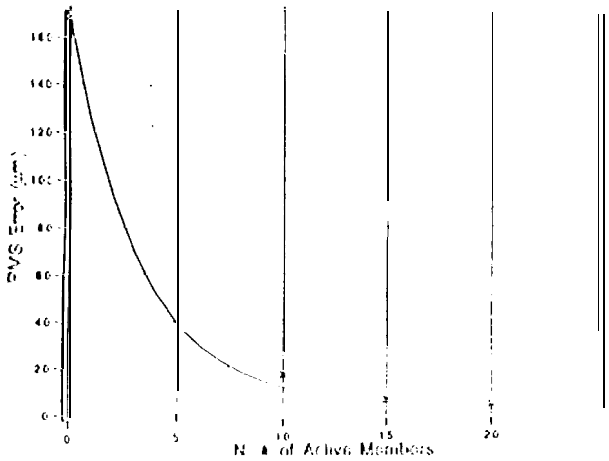

Figure 2. RMS Error Reduction with Increasing Number of Actuators

ii. From a practical point, one does not need to achieve the desired shape exactly, and therefore, one does not need to use a large number of actuators-even if the number of d.o.f. in the desired set is large. A remarkable degree of closeness to the rms error correction e, can be achieved by strategically replacing a small percentage of the total members by active members with optimized gains. For example, Fig. (2) shows that 47%, 70%, and 82% of the initial rms error can be corrected, respectively, with only two, four, and six of the total 150 members being active.

In view of the above results, the following experiments were designed to verify points on the curve in Fig. (2) which correspond to 2, 4, and 6 actuators.

III. Test Setup

1. Testbed Description: The testbed structure, shown in Fig. (1), is a support truss specifically designed and fabricated for a parabolic, 2.4 meter focal length, segmented reflector. The upper surface corner-to corner distance is nominally 3.9 meters. The thickness of the truss is approximately 0.64 meter. 150 Graphite-Epoxy struts, 300 aluminum erectable joint assemblies, and 45 aluminum nodes are used to construct a doubly curved tetrahedral truss. There are 27 nodes on the upper surface, and 18 nodes on the lower surface. The structure is supported at the three central nodes of the lower surface. The three support nodes are clamped to a 1130 kg steel block, which represents ground.

The erectable joint and node assembly design is a half scale version of the joint originally developed for Space Station Freedom. A detailed description of this joint can be found in Bush, et al [9]. The use of this type of joint allows for inspace erection of a precise, highly redundant structure. The key feature of the erectable joints is the sideways insertion of the strut into the truss. That is, the strut is placed into the truss by inserting the strut joint half sideways into the node joint half. The joint is then locked and lightly preloaded by a rotary cam mechanism that can be actuated by a simple turning of the joint cover. The joint halves at opposite ends of a strut have opposite thread directions, allowing the strut to be used as a turnbuckle. Prior to installation the strut length is precisely adjusted and locked into place by jam nuts. The nominal node center to node center lengths are 0.81350 meter for the core struts, range from 0.77147 to 0.81415 meters for the upper surface members, and range from 0.87716 to 0.91661 meters for the lower surface members. All lengths are set to within a tolerance of ±5 microns.

This testbed structure was extensively tested and characterized by both Bush, et al [9], and Umland and Lou [10]. One significant result of these characterization tests, was that the testbed was observed to have some nonlinearities, most likely arising from imperfect joints. A typical static deflection test result is shown in Fig. (3), where the rms of the distorted shape at the top surface is plotted versus the load applied at one of the corner nodes. Two complete load/unload cycles are displayed in the figure. Note that for the first load/unload cycle, the rms of the distortion does not return to zero when the load is removed, while for the second load/unload cycle the data points are nearly coincident - and when unloaded, the rms distortion returns to the new starting point.

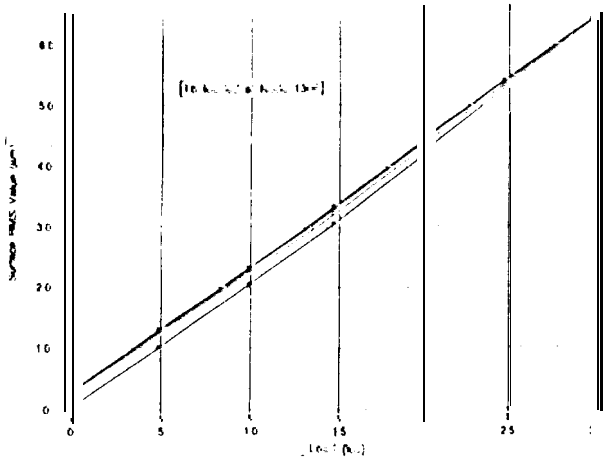

Figure 3. RMS Error for Corner Static Load

This suggests that there are joint nonlinearities which are being closed/opened when the structure is initially loaded, as well as angular reorientation of the joints. This will be discussed further in the test results.

2. **Actuators and Instrumentation:** The actuators used throughout the experiments are referred to as load screw active members. Each consists of a motorized micrometer as the primary component of the embeddable active member. The piezoelectrically driven active members previously developed and used at the Jet Propulsion Laboratory for adaptive studies are not suitable for the present static application because actuator gains (travel) on the order of 1 mm are required here. This exceeds the current capabilities of the piezoelectric strain - actuated active members. The motorized micrometer contains an M10x0.5 load screw driven by a DC gearmotor. The load screw active member assembly including the motorized micrometer, load cell, adapters, and erectable joints is shown in Fig. (4).

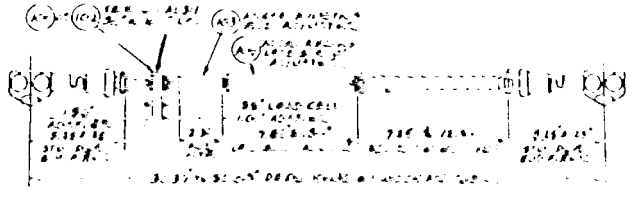

Figure 4. Load Screw Active Member

A Sensotec DC load cell is placed mechanically in series with each active member to measure the total load. Each load cell signal is conditioned by an Instrum amplifier. A magnetic encoder is incorporated into the gearmotor assembly. But due to rotational backlash of the gearhead, the encoder is a poor displacement transducer. Therefore, the DC load cell is used here as the feedback control sensor.

As in Ref. [10], the testbed is instrumented with fifteen Lucas-Schaevitz linear variable differential transformers (LVDT's) to measure the deflections in the Z-direction at the 15 nodes indicated in Fig. (5). These fall on the three major diameters of the upper surface of the testbed and serve as the control d.o.f. used in the analysis. This choice of locations was made here for easy access - not because of other functional requirements. The LVDT's are positioned in place from a relatively rigid support structure (known as gantry - not shown). The LVDT's are used with a signal conditioner whose bandwidth is 0-250 Hz. A low pass filter to minimize noise problems is also used. In addition to the LVDT's, the structure is instrumented with 14 thermocouples to monitor the temperature distribution across the upper surface and through the thickness of the structure.

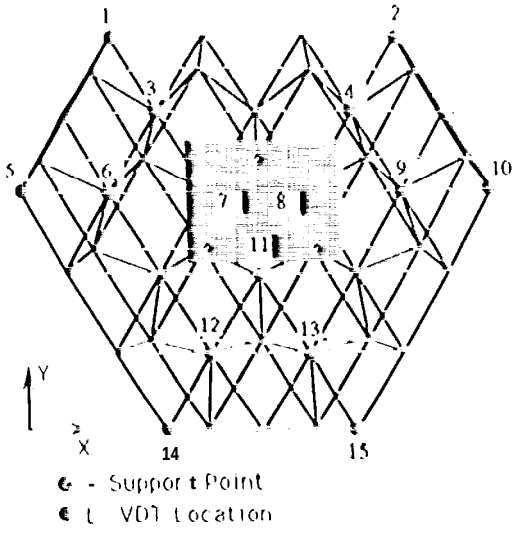

Figure 5. LVDT's at the Control d.o.f.

3. **Data Acquisition System:** To insure fast and accurate data recording, a data acquisition system (DAS) based on Labview software was used. During previous testing on the same structure [10],

it was found that differential thermal expansion between the testbed and the gantry produced an apparent drift on the instrumentation which obscured any structural nonlinearities. This drift is greatly minimized by the ability of the DAS to acquire the data quickly, so that the test is completed in as short time as possible. The DAS is capable of accepting outputs from all LVDT's, load cells, and thermocouples at once. It is also capable of initializing the test as required. This includes zeroing the LVDT signals, zeroing the load cell signals to give the member force due to the actuator, and recording the thermocouple readings as the test progresses. As the actuator forces are incrementally changed, the force - displacement data are acquired, averaged over multiple samples, and stored. The DAS is interfaced with a Microkinetics motor controller which operates either in a manual mode to incrementally change the force in the actuators, or in the automated actuator force control mode in which the maximum force in each actuator is given along with the number of increments to be used. In the latter mode, the DAS adjusts each actuator until the load cell associated with each actuator reads that the desired level has been achieved. An automatic override is built in the DAS, which will cause the system to shut down if the maximum force level is exceeded in any single load cell.

IV. Results of Experiments

As a demonstration of the adaptive shape control approach described in the analysis section, a series of validation tests were performed. They involved successive use of two, four, and six active members to distort the structure such that the deformation pattern, u, at the 15 - control d.o.f. closely approximates the deformation pattern, u^*, at the same d.o.f., had the structure been subjected to a prescribed thermal profile. This thermal profile was selected from the thermal analysis performed in Ref. [11] for the SMIM mission. It consists of a 5° K/m thermal gradient in the Y-direction, and no gradients in either the X or Z-direction. During testing, no thermal changes of any magnitude were intended to influence the structural deformation. In fact, the purpose of the thermocouples distributed throughout the structure was to monitor thermal changes - if any- from the beginning to the end of each test.

According to Eq. (1) and the analysis results of Fig. (2), u and u^* can be made closest in their rms sense if the two, four, or six active members were optimally located and their gains also optimized. These optimal locations are depicted in Fig. (6) and Table 1 for the two, four, and six groups of actuators. Notice that while the four actuator configuration is a subset of the six actuator configuration, the two actuator configuration is not. The corresponding optimal gains for each of the three configurations are also listed in Table 1, and the resultant Z-deformations at the control d.o.f. are given in Table 2. The results of Table 2 correspond to the 2, 4, and 6 actuator points on the curve of Fig. (2).

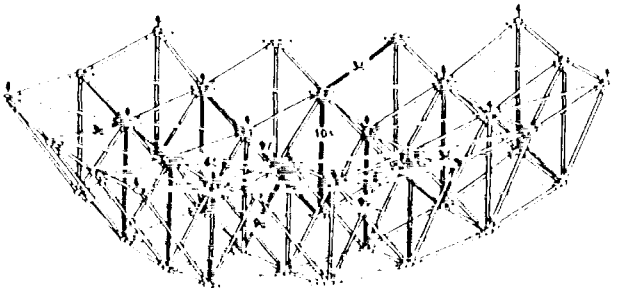

Figure 6. Optimal Actuator Locations

A series of 4 test configurations was conducted which include: (1) eight single actuators, (2) two actuators, (3) four actuators, and (4) six actuators. Prior to each test all load cells and displacement transducers were initialized to zero. Each test then involved commanding the actuators in question to adjust their lengths incrementally such that their load (measured by their load cells) reach the

Table 1. Optimal 2, 4, 6 Actuators and Their Gains

	2 Actuators	4 Actuators	6 Actuators
Actuator No.	38 103	34 97 98 99	34 36 64 97 98 99
Force (lb)	-s0.0 ???	-38.5 -46.0 -'4-/.0 -50.0	-33.9 -18.0 3.0 -46.7 -50.0 -46.9

Table 2. Deformations (microns) at Control D.O.F

Control D.O.F.	2 Actuators	4 Actuators	6 Actuators
1	-26.0	-28.0	-31.0
2	-32.0	-24.0	-29.0
3	-27.0	-23.0	-26.0
4	-24.0	-25.0	-27.0
5	-20.0	-16.0	-15.0
6	-20.0	-17.0	-19.0
4	- 5.6	-30.0	.31.0
8	- 4.3	-28.0	-27.0
9	-9.0	-19.0	-19.0
10	-7.9	-16.0	-16.0
11	+ 1.0	-21.0	-24.0
12	+ 0,7	- 2.8	. 5.0
13	+ 0.8	.4.4	.7,9
14	+ 4.-I	+ 4.0	+ 4.0
15	.0.7	+ 5.0	+ 3.5

maximum desired level. This was followed by incremental reversal of the loading in the actuators to the full magnitude but opposite sign, and then back to zero loads - also incrementally. In each loading/unloading direction ten increments were typically used. The forces in the actuators and corresponding displacements at the control d.o.f. are recorded at the end of each load increment. This cyclic load/unload procedure allowed observing any nonlinearities and/or residual, deformations remaining when the structure was completely unloaded.

The single actuator tests consisted of placing one actuator at a time at one of the 8 locations of Table 1 (also Fig. 6), then loading/unloading that actuator incrementally to ± 50 lb. Eight such tests were performed with the objective of characterizing the truss response. Essentially, these tests measured the S matrix of Eqs. (2) and (3), which is the actuators influence coefficients at the control points of interest. Figure (7) is an example of such experimental measurement of the influence coefficients for an actuator at location "97". Notice the small residual deformations of the order of 4 of 4 microns when the load in the member is completely removed. Other than this, the load deformation curve was typically linear. With this preliminary characterization, the following three tests aimed to emulate the analysis conditions in Table 1 for the two, four, and six actuators configurations. For example, in the two actuator test, one actuator was placed at location "38" and another placed at location "103" in Fig. (6). these two actuators were then incrementally loaded/unloaded simultaneously between (-50.0, 22.7) and (+ 50.0, -22.7) pounds.

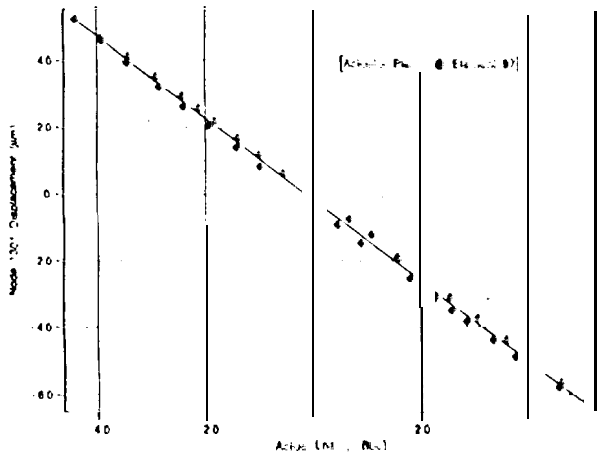

Figure 7. Influence Coefficient Measurement for Actuator at Location "97"

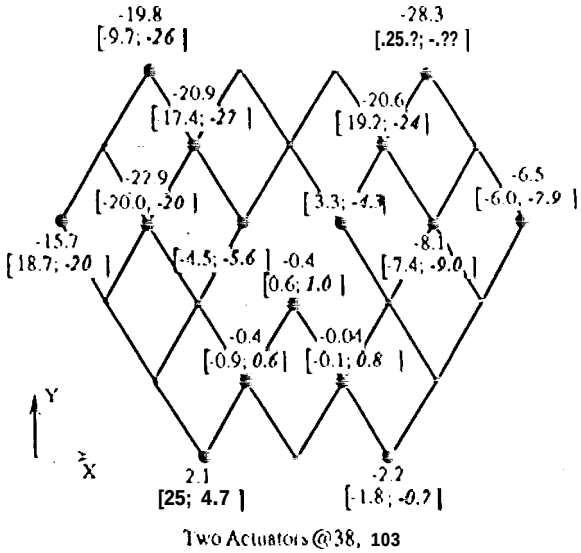

Figure 8. Test-Analysis Comparison for Two Actuators

The deformation at the 15 control d.o.f. for this test configuration are displayed in Fig. (8). The two values shown in each box correspond to results of the test and analysis (Table 1), respectively. The third value shown above each box was obtained by numerically combining the results of the appropriate single actuator tests. In the present case, these are the single actuator tests for location "38", and for location "103". This numerical combining of the two tests served to verify the influence coefficients that were experimentally measured from the single actuator tests. The two sets of experimentally derived values in Fig. (8) are rather consistent among themselves. And when compared with the analytical prediction of this case, one finds generally good agreements. Deviations on the order of 20% represent the norm. Based on previous testing this is expected. Another measure of the quality of agreement is the rms of the test deformations and analysis deformations. These were 47.8 and 63.4, respectively.

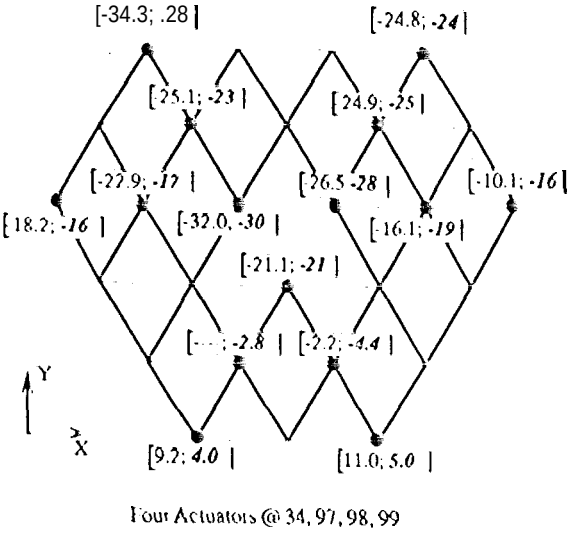

Figure 9. Test-Analysis Comparison for Four Actuators

Except for the number of actuators employed, their locations, and gains, the four actuator test configuration proceeded in the same manner as in the two actuators case. However, results of the four actuator tests (see Fig. 9) seem to compare more favorably with the analysis results than did the two actuators test. This is borne by comparing the individual response values at the control d.o.f., where deviations of the order of 7% were the norm. The rms values of the test and analysis deformations are 81.5 and 76.6, respectively.

The test procedure for the six actuators configuration was conducted similar to previous tests. Namely, beginning with the initially unloaded state, forces in the six actuators were incrementally and simultaneously applied up to their full (analytically derived) values in Table 1, then were incrementally reversed - passing through the unloaded state until they reached the negative of the same load levels of Table 1, and back to the initial unloaded state. The response of the structure at the maximum loading level is shown in Fig. (10) at the 15 control d.o.f. above each box. Results of the analytical simulation of this test conditions are indicated, also in Fig. (10), by the second set of values inside each box. Clearly, these two sets of results are in poor correlation.

At points of the loading path when the actuators were completely unloaded, residual deformation as large as 30 microns remained at some of the control d. o.f. The possibility that thermal changes that may have accrued over the test duration may have caused these deformations, was discounted on the basis of analysis of the thermal environment. Data recorded by the 14 thermocouples mounted throughout the structure, and showing thermal changes of the order of 0.5 °C was used in the analysis. The results indicated no more than 5 - 10 microns deformation at any d.o.f.

The only possible source for those residual deformations was believed to be inherent nonlinearities in the structure. And since the analysis assumed a linear elastic behavior, subtracting the residual deformations from the total observed values (above each box in Fig. 10) should provide a more rational basis for comparing the analysis and test results. As such, the corrected results are presented by the first value inside each box in Fig. (10). The blank spaces indicate no data due to failure of the LVDT's signal conditioners at those locations. The corrected test values shows greatly improved correlation with the analysis values but not as good as the correlations in the cases of single, two, and four actuators. The rms of the corrected test deformations are now 88.4 in comparison with 78.9 for the rms of the analysis deformations.

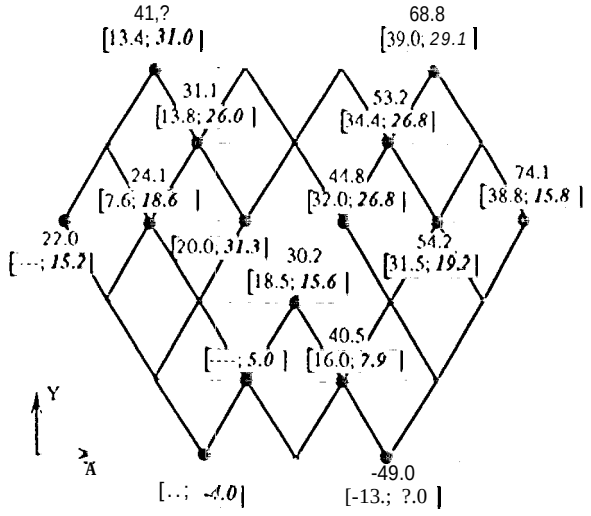

Figure 10. Test-Analysis Comparison for Six Actuators

In absence of additional testing to study the observed nonlinearities, one can only speculate as to their source and nature. During previous testing of this structure [9], only linear behavior was observed. In the present tests anti in Ref. [1 O] deformations were on the micron level. Nonlinearities of different magnitude were observed both in Ref. [10] e.g. see Fig. (1) and in the present tests. In spite of the fact that joints of the testbed truss were specially designed and built to a high degree of precision, they appear to be a strong suspect for causing the observed micron level nonlinearities. Coupled with random variations in the geometric dimensions of the truss members, and angular tolerances in the orientation of the various members meeting at a joint, it is plausible that small nonlinearities in some of the joints would react preferentially depending 011 the load distribution throughout the truss. This may explain the small residual deformations (of order 5 microns) in case of the single, two, and four activators - while the relatively localized loading could excercise few nonlinear joints, as compared to the residual deformation of up to 30 microns in the six actuators case where loading was more distributed and could have dominance over a larger number of nonlinear joints.

But aside from discovering such nonlinearities, the present tests correlated reasonably well with the analysis results. Had the structure been perfectly linear, the tests confirmed that a limited number of strategically placed active members could indeed be used to correct shape aberrations.

V. Conclusion

Using a realistic space erectable truss structure, results of the tests described therein demonstrated the ability of a limited number of active members to produce the desired shape corrections with reasonable accuracy. In a series of tests, successively increasing number of actuators were used to produce a desired pattern of shape corrections. Correlations with analytical predictions were good under all test conditions where nonlinearities were negligible.

In the six actuators test, residual deformations of up to 30 microns were observed when all actuators were completely unloaded, most probably due to nonlinearities in the joints. Apparently, these nonlinearities were not exhibited when the same structure was previously tested. And although these micron level nonlinearities obscured an otherwise good correlation with the linear analysis, their observation here adds special significance to the use of adaptive concepts in precision structures.

Adaptive concepts are especially aimed at such sources of uncertainties in behavior. In a closed loop system, once those residual deformations are sensed, they can be corrected adaptively by the active members to any desired degree of accuracy. The use of active members in precisions structures can also ease, and in fact may provide an attractive alternative to requirements that certain structural or optical components be constructed from 100% dimensionally stable materials.

VI. ACKNOWLEDGEMENT

The research described therein was performed at the Jet Propulsion Laboratory, California Institute of Technology, under contract with the National Aeronautics and Space Administration. The assistance of several co workers in this effort is gratefully acknowledged. They include R. Helms, R. Losey, C. Miller, and D. Moore.

V I I . REF E RE NCES

1. Padula, S.L , Adelman, H.M., and Bailey, M. C., "Integrated Structure Electromagnetic Optimization of Large Space Antenna Reflector," NASA 1 M-89110, f ebruary 1987.

2. Burdisso, R.A. and t lafika, R.T., "Optimal Location of Actuators for Correcting Distortions in 1 arge Truss Structures," AIAA Journal, Vol. 27, No. 10, October 1 989, pp. 14(X1411.

3. } lafika, R.T. and Adelman, t I.M., "Damping and Control of Spacecraft Structures: Selection of Actuator Locations for Static Shapo Control of Large Space Structures by t leuristic Integer Programming," Comp rotor and Structures, Vol. 20, No. 1-3, 1985, pp. 575 582.

4. Chen, G-S., Bruno, R., and Salama, M . , "Optimal Placement of Active/Passive Members in Truss Structures Using Simulated Annealing," AIAA Journal, Vol 29, No. 8, August 1991, pp. 1327-1334.

5. Bruno, R., Salama, M., and Garba, J., "Actuator Placemont for Static Shapo Control of Nonlinear 1 russ Structures," Proceedings of the 1 hird International Conference on Adaptive Structures, San Diogo, CA, November 1 992.

6. Das, S.K., Utku, S., Chon, G-S., and Wada, B.K., 'A Mathematical Basis for tho Design and Design Optimization of Adaptive 1 russes in Precision Control," Proceedings of the F irst Joint U.S./Japan Conference on Adap tive Structures, November 1990, Maui, t II, pp. 660-688.

7. Kuo, C.P. and Bruno, R., "Optim al Actuator Placemont in an Active Reflector Using a Modified Simulated Annealing 1 echnique, Proceedings of tho First U. S./Japan Conference on Adaptive Structures, Maui, t II, pp. 1056. 1067.

8. Tabata, M. et al, "Shapo Control E xperiments with a F unctional Modol for Large Optical Reflectors," Proceedings of the f irst Joint U. S./Japan Conference on Adaptive Structures, November 1990, Maui, HI, pp. 615-630.

9. Bush, H.G., et al, "Design and F abrication of an E rectat ble T russ for Precision Segmented Reflector Application,' AIAA Paper 90 0999, 31st AIAA/ASME /ASCE /A} IS/ASC Structures, Structural Dynamics, and Materials Conference, Long Beach, CA, April 1990.

1 Cr. Umland, J.W. and Lou, M. G., "Precision Segmented Reflector Primary Support Structural Testing," AIAA Paper 92-2535, 33rd AIAA/ASME /AHS/ASC Structures, Structural Dynamics, and Materials Conference, Dallas, 1X, April 1992,

11, Tsuyuki, G. and Mahoney, M. J., '-1 ho f'recision Segm ented Reflector Program: On-Orbit Behavior of tho Submillimeter Imager and L ino Survey Telescope," AIM 261111 hermophysics Conference, Honolulu, HI, June 1991.